

*Supporting information for*

Impact of hydrophobicity on local solvation structures and its  
connections with global solubilization thermodynamics of amphiphilic  
molecules

Bibhab Bandhu Majumdar<sup>1†</sup>, Partha Pyne<sup>1</sup>, Rajib Kumar Mitra<sup>1\*</sup>, and Debasish  
Das Mahanta<sup>2,‡,\*</sup>

<sup>1</sup>Department of Chemical and Biological Sciences; S. N. Bose National Centre for Basic  
Sciences; Block-JD; Sector-III; Salt Lake; Kolkata-700106, INDIA

<sup>2</sup>Department of Chemistry, The University of Texas at Austin, 105 E 24th 4 Street, Austin,  
TX 78712, USA

<sup>†</sup>Present Address: VIT University Andhra Pradesh, Amaravati, 522237 Andhra Pradesh,  
INDIA

<sup>‡</sup>Present address: Department of Physics, Gandhi Institute of Technology and Management  
(GITAM), Bengaluru, Karnataka 561203, INDIA

\*Email: [rajib@bose.res.in](mailto:rajib@bose.res.in) (RKM); [snbdebasish@gmail.com](mailto:snbdebasish@gmail.com) (DDM)

## Experimental methodology

*Far infrared (FIR) measurements:* Far-IR spectra were collected in ATR unit and were converted into absorbance using the following relation,

$$Abs(\nu) = \frac{\text{intensity in ATR unit} \times 1000}{\text{wave number}} \quad (1)$$

The frequency dependent absorption coefficient,  $\alpha(\nu)$  was estimated as

$$\alpha_{\text{solution}}(\nu) = \frac{Abs_{\text{solution}}(\nu) - Abs_{\text{air}}(\nu)}{d_p} \quad (2)$$

where  $d_p$  is the penetration depth<sup>1</sup> defined as

$$d_p = \frac{\lambda}{2\pi \sqrt{(n_d \sin\theta)^2 - n_s^2}} \quad (3)$$

where  $\lambda$  is the wavelength of the radiation;  $n_d$  and  $n_s$  are the refractive indices of the diamond crystal and the sample, respectively.  $\theta$  is the incidence angle (here  $\theta = \frac{\pi}{4}$ ). To get rid of the bulk contributions from  $\alpha_{\text{solution}}$  we calculate the difference in the absorption  $\Delta\alpha(\nu)$  by subtracting the density corrected spectrum of pure water and pure alcohol using the following equation,<sup>2-4</sup>

$$\Delta\alpha(\nu) = \alpha_{\text{solution}}(\nu) - \zeta_{\text{water}}\alpha_{\text{water}} - \zeta_{\text{alc}}\alpha_{\text{alc}} \quad (4)$$

where  $\zeta_{\text{water}}$  and  $\zeta_{\text{alc}}$  are the correction factor for water and alcohol, respectively. We fit the  $\Delta\alpha(\nu)$  profile using a sum of three damped harmonic oscillator model<sup>5</sup>

$$\Delta\alpha(\nu) = \sum_{i=1}^2 \frac{a_i \omega_i \nu^2}{\nu^2 \omega_i^2 + \pi^2 \left( \nu_i^2 + \frac{\omega_i^2}{4\pi^2} - \nu^2 \right)^2} \quad (5)$$

where  $a_i$ ,  $\omega_i$ ,  $\nu_i$  are the amplitude, width, and the centre frequency for the  $i^{\text{th}}$  resonance. The unperturbed centre frequency is defined as,

$$v_{0,i} = \sqrt{v_i^2 + \frac{\omega_i^2}{4\pi^2}} \quad (6)$$

*THz time-domain spectroscopy (TTDS) measurement:* TTDS measurements were carried out in a commercially available TeraSmart spectrometer (Menlo System). A 1560 nm laser having a pulse width of <90 fs and a repetition rate of 100 MHz was used to excite a THz emitter antenna (TERA 15-FC), producing THz radiation with a bandwidth of up to 3.0 THz (460 dB). This THz radiation was then focused on the sample, and the transmitted THz radiation was further focused on a THz detector antenna (TERA 15-FC), which is gated by the probe laser beam. The frequency dependent (0.3-2 THz) amplitude and phase of the transmitted pulse was obtained by using Fourier analysis of the measured electric field amplitude  $E_{\text{THz}}(t)$ . With a coherent detection mechanism TTDS can measure both amplitude and phase of the radiation in a single measurement and thus can provide information on frequency dependent optical parameters of the solutions. The absorption coefficient  $\alpha(\nu)$  is calculated with the Beer-Lambert law,

$$\alpha(\nu) = \frac{1}{d} \ln \frac{I_o}{I} \quad (7)$$

where  $d$  is the thickness of the sample,  $I$  and  $I_o$  are the transmitted signal passing through sample and reference respectively. The frequency dependent real ( $\epsilon_{re}$ ) and imaginary ( $\epsilon_{im}$ ) dielectric constants of the samples are extracted as,  $\epsilon_{re} = n^2(\nu) - k^2(\nu)$  and  $\epsilon_{im} = 2n(\nu)k(\nu)$ , where the complex refractive index is given as:  $\tilde{n}(\nu) = n(\nu) - ik(\nu)$ , with  $k(\nu) = c\alpha_{\text{THz}}(\nu)/4\pi\nu$ ;  $c$  being the speed of light. The complex dielectric function  $\tilde{\epsilon}(\nu) = \epsilon_{re}(\nu) - i\epsilon_{im}(\nu)$  is fitted with a multicomponent Debye relaxation model, given by

$$\tilde{\epsilon}(\nu) = \epsilon_{\infty} + \sum_{j=1}^3 \frac{\epsilon_j - \epsilon_{j+1}}{1 + 2\pi i \nu \tau_j} \quad (8)$$

where  $\tau_j$  is the relaxation time of  $j^{\text{th}}$  mode and  $\epsilon_j$  is the dielectric constants of the corresponding modes.  $\epsilon_{\infty}$  is the extrapolated dielectric constant at the very high frequency and  $\nu$  is the frequency.

*H-bond Analysis protocol from MD simulations:* We tagged each individual water molecules in the simulation box and assigned two flag variables  $\text{flagH1}(i,t)$  and  $\text{flagH2}(i,t)$ , where “i”

represents the index of water molecule and “t” is the temporal coordinate or the frame number. These flag matrices were computed from the coordinates of the MD trajectory and have a dimension of ( $n_w$  x time), where  $n_w$  and time refers to the number of water molecules and corresponding frame number, respectively. We have used the most conventional geometrical HB definition (scheme 1) which consists of three criteria: (i) for alcohol-water (between hydroxyl oxygen of alcohol and oxygen of water;  $O_{alc}-O_w$ ) and for water-water (between the oxygens of two water molecules;  $O_w-O_w$ ) cut-off distances should be less than 0.35 nm and 0.30 nm, respectively, (ii) the vector distances  $O_{alc}-H_w$  (for alcohol-water HB) and  $O_w-H_w$  (for water-water HB) should be below 0.20 nm and (iii) the cut-off angle (between the OH vector of any water and the vector joining the two -O atoms of water-water or water-alcohol partners) should be less than  $\pi/6$  radians ( $30^\circ$ ). The alcohol-water and water-water distance cut-off limits were fixed from the first minimum of their respective radial distribution functions (RDF). We allocated flagH1(i,t) to a value j, if the ith water molecule donates a HB to the jth water molecule or  $j + n_w$ , if it is HB to the jth alcohol molecule at time t via H1 (one of the H-atoms of molecule “i”). If the ith water molecule does not donate a HB to any other molecule through H1, this flag is assigned a value of zero. Similar procedure is followed for the other H-atom, H2 of molecule “i” to construct the flagH2 matrix as well. All the other parameters associated with the HB-conformations are calculated further from these two flag matrices.

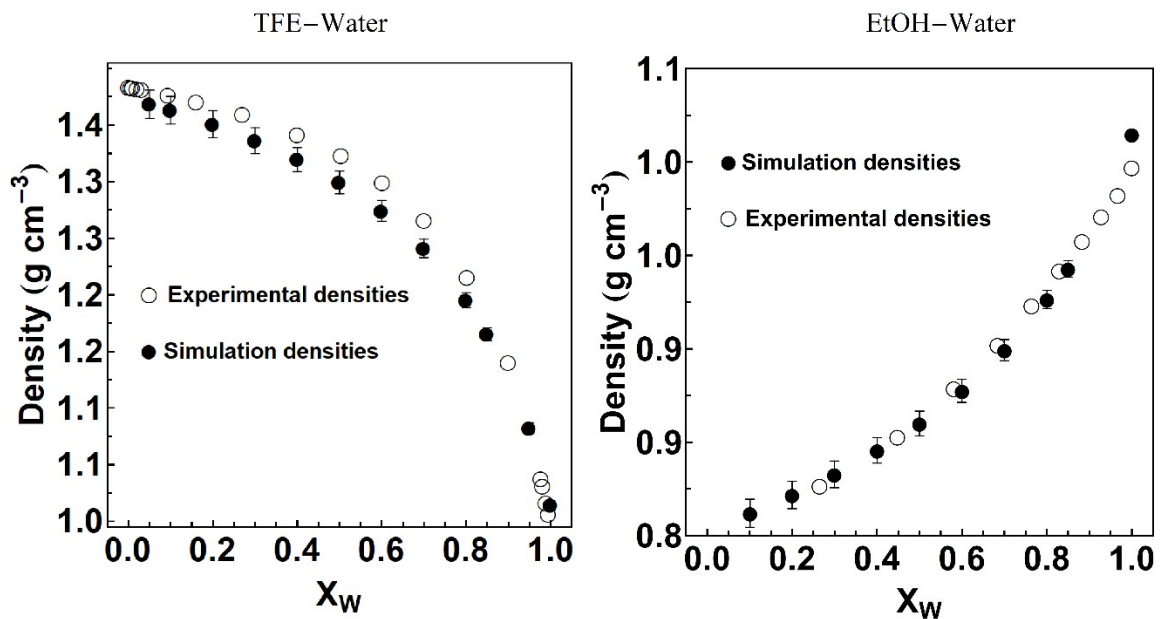


**Figure S1.** Comparison of mixture densities as obtained from simulation (filled black circles) and the previously reported experiment values (open circles) for TFE-water (in left panel) and EtOH-water (in right panel) binary mixtures. Standard deviations of the individual density values obtained from MD simulation are shown by vertical lines on top of individual data points.

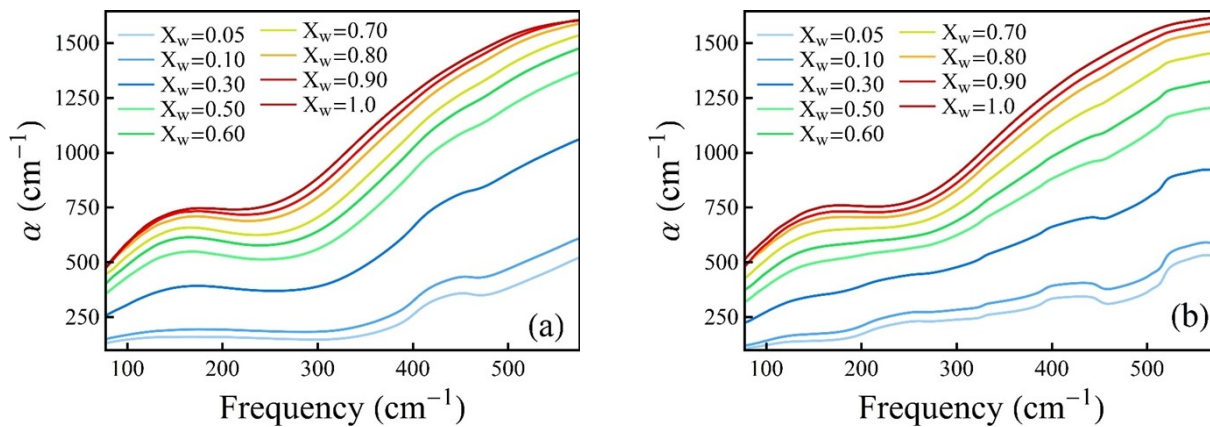


**Figure S2:** (a) Frequency dependent THz absorption spectrum coefficient,  $\alpha(\nu)$  of (a) EtOH-water and (b) TFE-water binary mixtures with varying water content ( $X_w$ ).

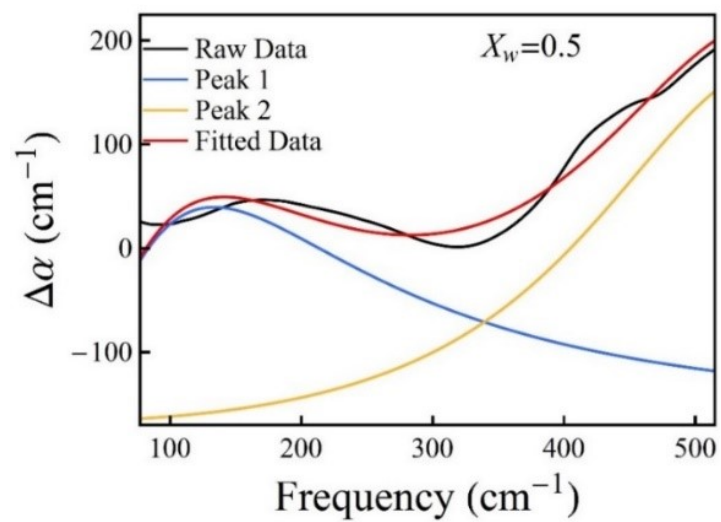


**Figure S3.** Representative fitting of the difference absorption spectra measured with FIR/THz experiments.

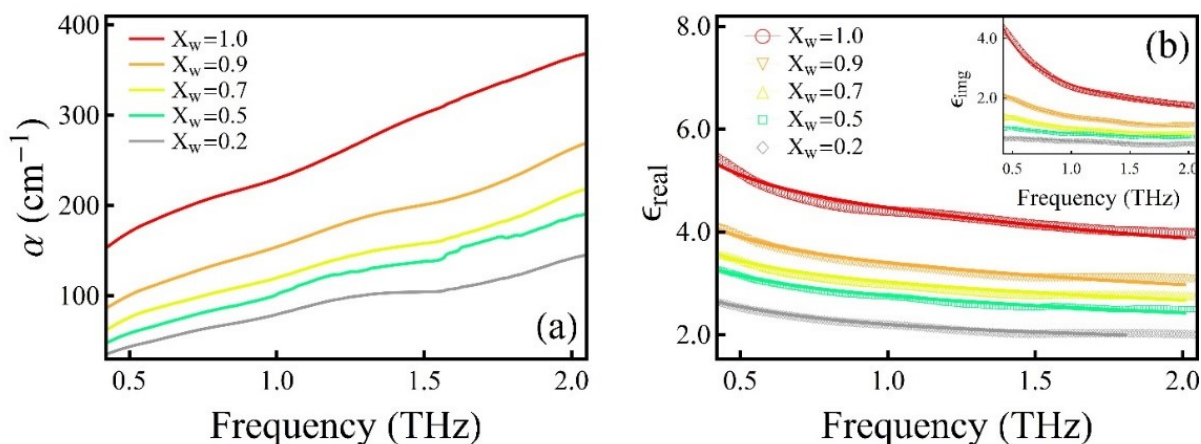


**Figure S4:** Representative profile of  $\alpha(\nu)$  with varying EtOH content in the solution as obtained from THz-TDS measurements. (b) Representative profile of  $\epsilon(\nu)$  with varying EtOH content in the solution. Inset represent the imaginary profile.

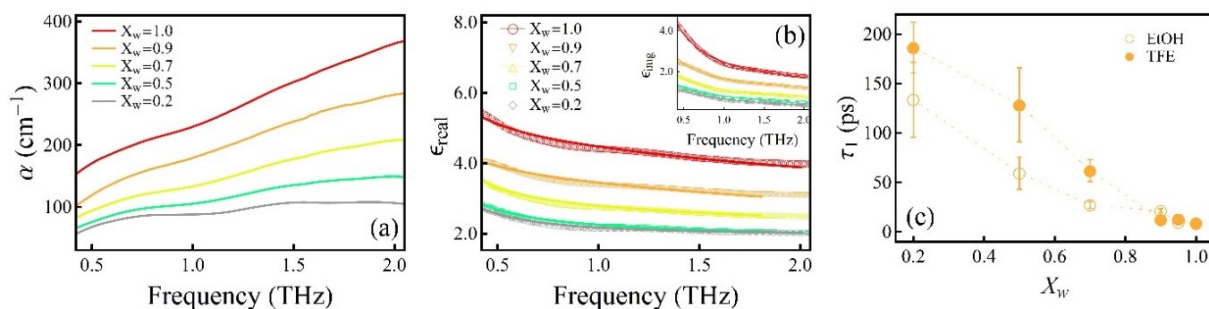


**Figure S5.** (a) Representative profile of  $\alpha(\nu)$  with varying TFE content in the solution as obtained from TTDS measurements. (b) Representative profile of  $\epsilon(\nu)$  with varying TFE content in the solution. Inset represent the imaginary profile. (c) time scales associated with cooperative rearrangement of H-bond network for both EtOH and TFE aqueous solutions respectively as obtained from the Debye fitting of dielectric constants.

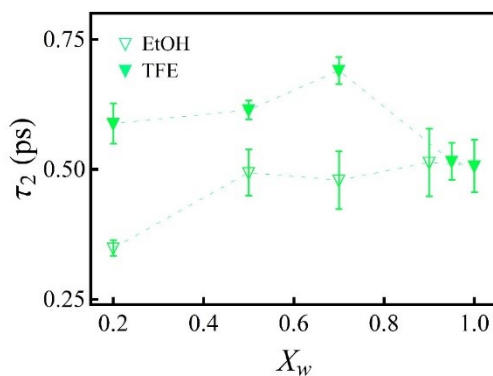


**Figure S6:** Change in  $\tau_2$  with  $X_w$ , for both EtOH and TFE respectively as obtained from the Debye fitting of dielectric constants.

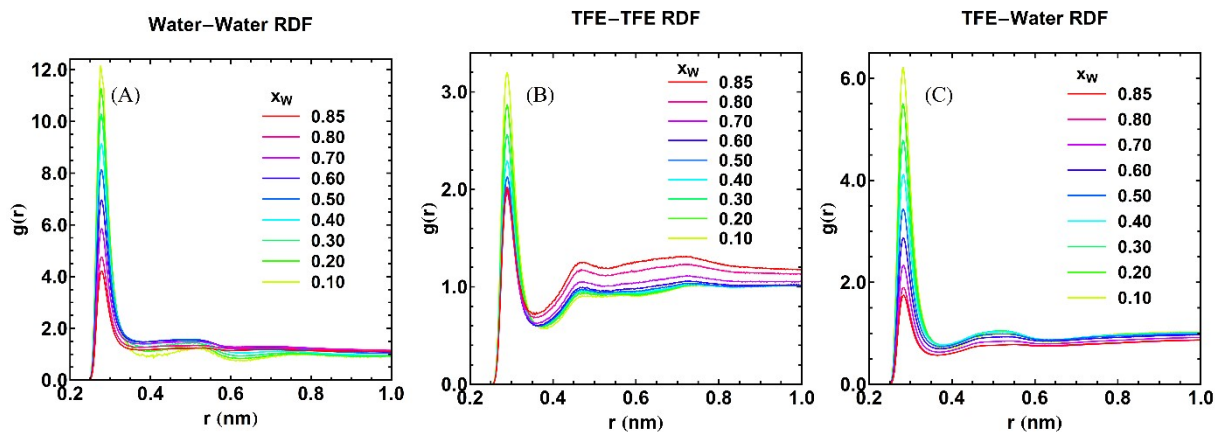


**Figure S7:** Radial distribution functions are plotted for (A) homo-molecular; water-water, cross-molecular (B) TFE-TFE and (C) TFE-water interactions, respectively in TFE-water binary mixtures at various  $X_w$ :

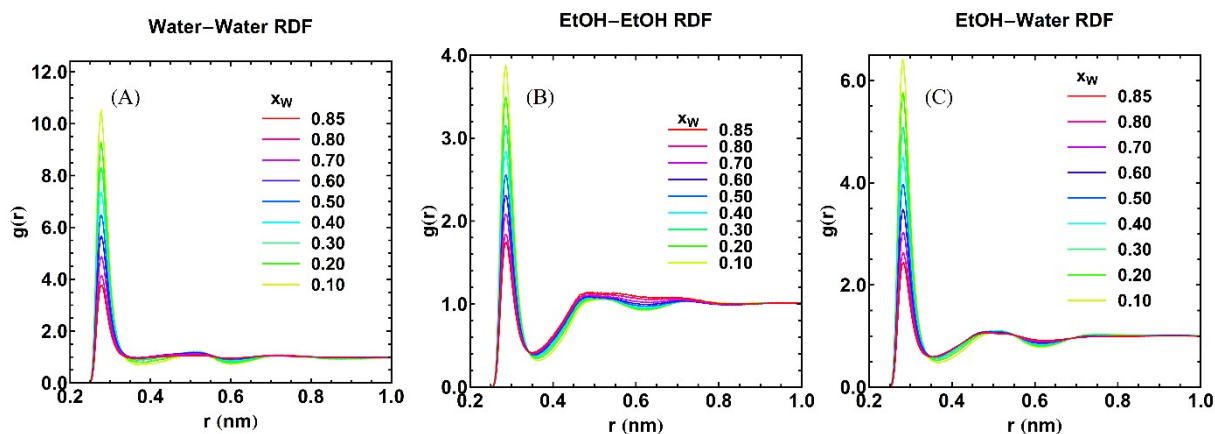


**Figure S8:** Radial distribution functions are plotted for (A) homo-molecular; water-water, cross-molecular (B) EtOH-EtOH and (C) EtOH-water interactions, respectively in EtOH-water binary mixtures at various  $X_w$ .

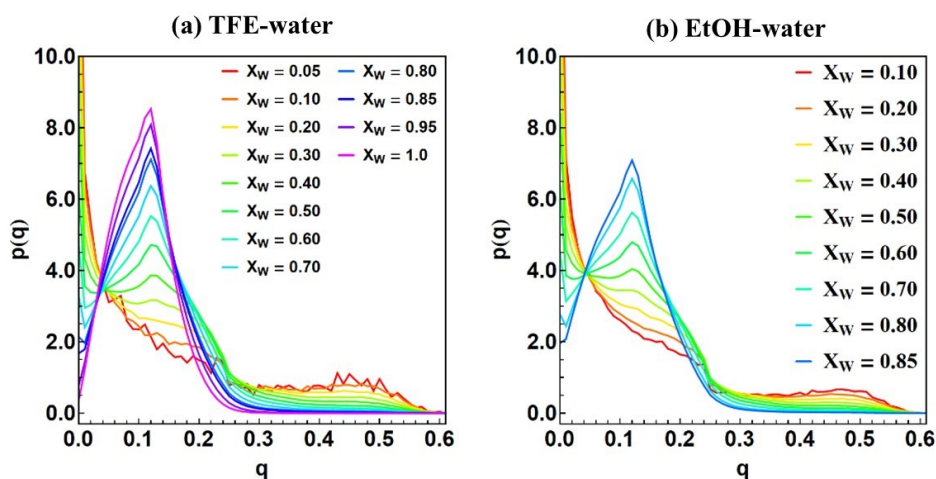
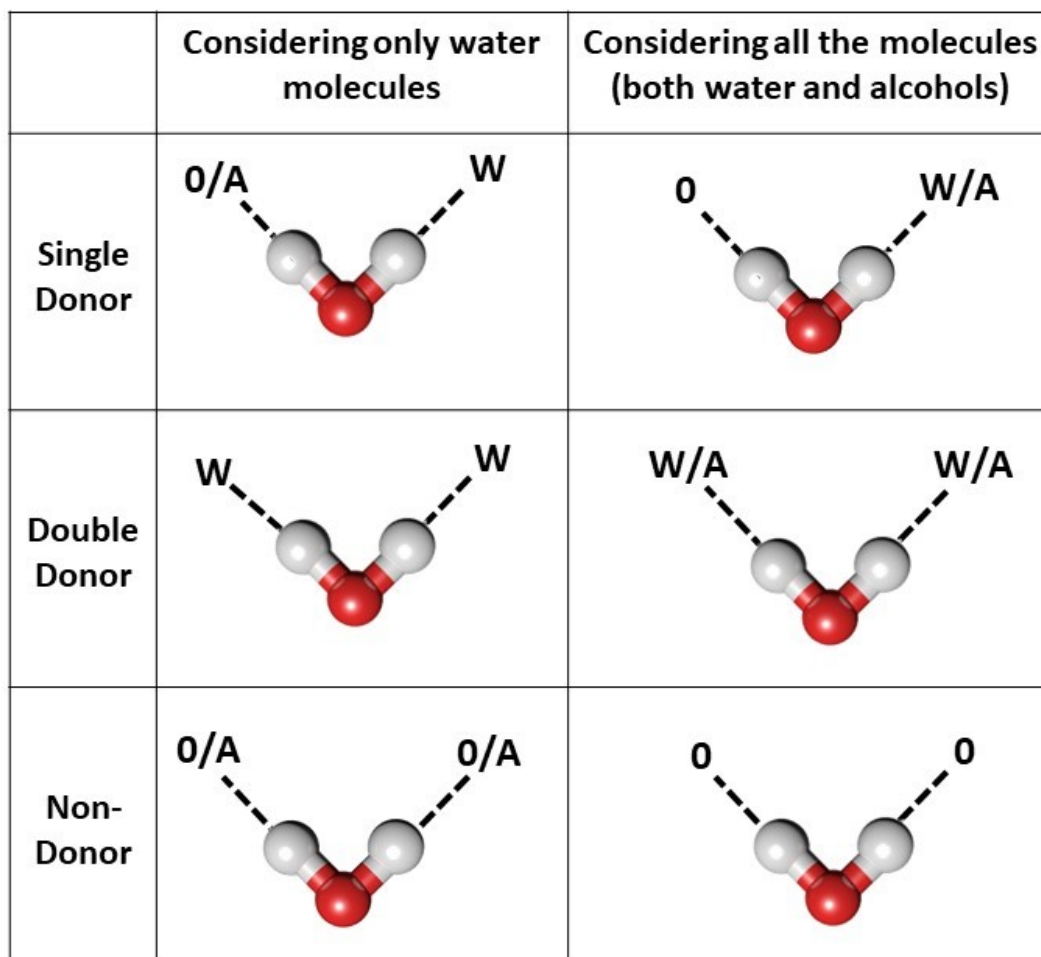


**Figure S9:** Water tetrahedral order parameter ( $q$ ) distribution:  $p(q)$  obtained from MD simulations at various water mole fractions for (a) TFE-water and (b) EtOH-water binary mixtures, respectively.



**Scheme S1.** Schematic representation of the various types of HB configuration of water; (a) single donor, (b) double donor, and (c) non-HB donors by considering all the molecules (both alcohol and water) in the simulation box. The centre donor water molecule is represented with a red and white colour while the HB acceptors O/A/W represents null/alcohol/water molecules.

**Table S1.** Fitting parameters of the experimental FTIR-FIR spectra the alcohol-water mixtures.

$X_w$	$A_{HB}$	$\nu_{HB}$ (cm <sup>-1</sup> )	$A_{Lib}$	$\nu_{Lib}$ (cm <sup>-1</sup> )
<b>EtOH-water</b>				
0.1	48433±3624	110±13	352527±42223	588±11
0.2	50202±3387	119±12	338771±28229	566±7
0.3	54761±3358	130±10	360154±22629	555±5
0.4	59288±3227	148±7	400542±21074	551±4
0.5	67713±3184	156±5	472633±21066	549±4
0.6	69615±2975	160±5	507364±20512	548±4
0.65	71398±2980	158±5	521887±20685	548±4
0.7	71861±2882	156±5	525829±20065	547±4
0.75	67983±2569	156±5	526737±19434	548±4
0.8	77144±2555	146±4	577605±19959	549±4
0.85	77138±2325	142±4	561532±18450	550±4
0.9	56780±1829	139±5	407125±14139	548±4
<b>TFE-water</b>				
0.2	4892 ± 520	249 ± 3	3858 ± 591	363 ± 7
0.3	10287 ± 1123	245 ± 3	15713 ± 1561	392 ± 10
0.4	11094 ± 1516	243 ± 3	20798 ± 2357	388 ± 15
0.5	15862 ± 1980	242 ± 3	32911 ± 4395	436 ± 23
0.6	43400 ± 1325	265 ± 4	16473 ± 905	506 ± 1
0.65	48594 ± 1310	256 ± 4	23480 ± 968	511 ± 2
0.7	66922 ± 2069	242 ± 6	41703 ± 1599	515 ± 1
0.75	62546 ± 1822	225 ± 6	51703 ± 1690	519 ± 1
0.8	45160 ± 1083	205 ± 4	55123 ± 1382	521 ± 1

**Table S2.** Dielectric relaxation fitting parameters for alcohol-water solutions

System ( $X_w$ )	${}^6\epsilon_s$	$\epsilon_1$	$\epsilon_2$	$\epsilon_\infty$	$\tau_1$ (ps)	$\tau_2$ (ps)	$\tau_3$ (ps)*
<b>EtOH-water</b>							
1	78.0	6.46	4.55	3.02	$8.63 \pm 0.21$	$0.51 \pm 0.05$	0.075
0.95	73.0	5.73	4.06	2.93	$9.58 \pm 0.18$	$0.33 \pm 0.02$	0.075
0.9	65.0	5.29	3.42	2.37	$21.19 \pm 2.09$	$0.51 \pm 0.06$	0.075
0.7	47.7	4.49	3.03	2.19	$27.16 \pm 3.46$	$0.47 \pm 0.05$	0.075
0.5	37.0	4.19	2.77	1.96	$59.33 \pm 16.30$	$0.49 \pm 0.04$	0.075
0.2	28.0	3.13	2.09	1.71	$133.65 \pm 37.92$	$0.34 \pm 0.01$	0.075
<b>TFE-water</b>							
0.95	73.2	7.03	4.56	3.25	$12.96 \pm 0.44$	$0.52 \pm 0.04$	0.0075
0.9	65.0	4.73	3.53	2.28	$12.55 \pm 0.73$	$0.44 \pm 0.08$	0.075
0.7	48.0	6.18	2.74	2.07	$61.94 \pm 11.10$	$0.69 \pm 0.03$	0.075
0.5	37.0	4.74	2.15	1.82	$128.54 \pm 37.55$	$0.61 \pm 0.02$	0.075
0.2	28.0	4.39	2.03	1.94	$186.59 \pm 25.58$	$0.59 \pm 0.04$	0.075

**Table S3.** Details of the simulated TFE-water mixtures.

$X_w$	$N_w$	$N_{TFE}$	Box length (nm)	Densities (g/cm <sup>3</sup> )
0.05	21	400	3.66	1.368
0.1	45	400	3.68	1.363
0.2	100	400	3.72	1.350
0.3	171	400	3.77	1.336
0.4	267	400	3.83	1.319
0.5	400	400	3.92	1.299
0.6	600	400	4.05	1.274
0.7	934	400	4.24	1.241
0.8	1600	400	4.57	1.195
0.85	2267	400	4.87	1.165
0.95	3345	180	4.93	1.082
1.0	4069	0	4.93	1.014

**Table S4.** Details of the simulated EtOH-water mixtures.

$X_w$	$N_w$	$N_{Eth}$	Box length (nm)	Densities (g/cm <sup>3</sup> )
0.1	45	400	3.45	0.811
0.2	100	400	3.49	0.821
0.3	171	400	3.50	0.832
0.4	267	400	3.57	0.845
0.5	400	400	3.67	0.860
0.6	600	400	3.81	0.877
0.7	934	400	4.02	0.899
0.8	1600	400	4.39	0.926
0.85	2267	400	4.70	0.942

**Table S5.** Hydrogen-bond lifetimes (in picoseconds) for different *homo-molecular* and *hetero-molecular* H-bonded species in TFE-water binary mixtures.

$X_w$	water-water	HB lifetime (ps) TFE-TFE	HB lifetime (ps) TFE-water
0.30	10.44	9.46	10.70
0.50	6.50	8.03	7.83
0.70	4.25	7.12	6.04
0.85	3.25	6.17	4.63

**Table S6.** Hydrogen-bond lifetimes (in picoseconds) for different *homo-molecular* and *hetero-molecular* H-bonded species in EtOH-water binary mixtures.

$X_w$	water-water	HB lifetime (ps) EtOH-EtOH	HB lifetime (ps) EtOH-Water
0.30	17.26	18.98	17.90
0.50	11.12	13.89	12.21
0.70	8.80	9.57	7.74
0.85	6.81	6.29	5.10

## References

1. Milosevic, M., Internal Reflection and ATR Spectroscopy. *Applied Spectroscopy Reviews* **2004**, 39 (3), 365-384.
2. Chakraborty, S.; Pyne, P.; Kumar Mitra, R.; Das Mahanta, D., A subtle interplay between hydrophilic and hydrophobic hydration governs butanol (de)mixing in water. *Chemical Physics Letters* **2022**, 140080.
3. Das Mahanta, D.; Brown, D. R.; Pezzotti, S.; Han, S.; Schwaab, G.; Shell, M. S.; Havenith, M., Local solvation structures govern the mixing thermodynamics of glycerol–water solutions. *Chemical Science* **2023**, 14 (26), 7381-7392.
4. Chakraborty, S.; Pyne, P.; Mitra, R. K.; Das Mahanta, D., Hydrogen bond structure and associated dynamics in micro-heterogeneous and in phase separated alcohol-water binary mixtures: A THz spectroscopic investigation. *Journal of Molecular Liquids* **2023**, 382, 121998.
5. Dodo, T.; Sugawa, M.; Nonaka, E.; Honda, H.; Ikawa, S. i., Absorption of far-infrared radiation by alkali halide aqueous solutions. *The Journal of Chemical Physics* **1995**, 102 (15), 6208-6211.
6. Sato, T.; Buchner, R., Dielectric Relaxation Processes in Ethanol/Water Mixtures. *The Journal of Physical Chemistry A* **2004**, 108 (23), 5007-5015.